Tetrahedron: *Asymmetry* xxx (2015) xxx–xxx

Contents lists available at ScienceDirect

Tetrahedron: *Asymmetry*

journal homepage: www.elsevier.com/locate/tetasy

Asymmetric synthesis approach of enantiomerically pure spiro-indenoquinoxaline pyrrolidines and spiro-indenoquinoxaline pyrrolizidines

Naeimeh Shahrestani [a], Farbod Salahi [a], Niloofar Tavakoli [a], Khosrow Jadidi [a,*], Mahshid Hamzehloueian [b], Behrouz Notash [a]

[a] *Department of Chemistry, Shahid Beheshti University, G.C., Tehran 1983963113, Iran*
[b] *Department of Chemistry, Islamic Azad University, Jouybar Branch, Jouybar 47715-195, Iran*

ARTICLE INFO

Article history:
Received 12 December 2014
Revised 14 August 2015
Accepted 18 August 2015
Available online xxxx

ABSTRACT

An efficient, one-pot, four-component procedure for the synthesis of a small library of novel chiral spiro-indenoquinoxaline pyrrolidines and chiral spiro-indenoquinoxaline pyrrolizidines with high regio-, diastereo- (up to 96 dr), and enantioselectivity (up to 99% ee), through a 1,3-dipolar cycloaddition reaction of azomethine ylides and an optically active cinnamoyl–crotonoyl oxazolidinone is described. This methodology was very simple and was utilized to construct complex products from simple starting materials. The process was carried out in aqueous ethanol as an eco-friendly solvent and in the absence of any Lewis acids catalysts. The oxazolidinone chiral auxiliary was removed through a non-destructive protocol. The reaction mechanism is discussed on the basis of the assignment of the absolute configuration of the cycloadducts and using quantum mechanical calculations. The regio- and stereoselectivity were described on the basis of transition states' stabilities and global and local reactivity indices of the reactants. The results of the theoretical calculations are in agreement with the experimental outcomes.

© 2015 Elsevier Ltd. All rights reserved.

1. Introduction

The advantages of asymmetric multicomponent reactions together with the high level of stereoselectivity attained in some of these reactions, have forced chemists in industry and in academia to adopt this new synthesis strategy as a viable option.[1]

Asymmetric 1,3-dipolar cycloaddition reactions have become a rapidly growing field of research in organic chemistry. This approach allows the chirality in a product to be introduced via attachment and removal of a chiral auxiliary. A number of asymmetric 1,3-dipolar cycloaddition reactions of azomethine ylides, where the chirality was located in the dipolarophile using a chiral auxiliary, are described in the literature.[2–4]

Asymmetric 1,3-dipolar cycloaddition reactions of azomethine ylides offer an effective approach to access chiral pyrrolidines and pyrrolizidines substructures containing three or four new stereogenic centres that are found in many biologically active compounds,[5,6,7a,b] particularly for spiro-pyrrolidines that exhibit anticonvulsion[7c] potential antileukaemic[7d] local anaesthetic[7e] and antiviral activities.[7f] In addition, tetracyclic indenoquinoxalines are important types of nitrogen containing heterocyclic compounds, which have both biological and pharmaceutical properties.[8] For example, quinoxalines, brimonidine and varenicline (Fig. 1) have been approved by the food and drug administration for the treatment of glaucoma[9a] and smoking cessation therapy,[9b,c] while NVPBSK805,[9d] NCGC55879-01[9e] and R(+) XK469,[9f] act as potent janus kinase inhibitors, BRCA1 inhibitors and anti-tumour agents, respectively.

It is expected that joining indenoquinoxaline to a chiral pyrrolidine or pyrrolizidine ring through a spiro atom at the C-3 position could lead to the formation of chiral spiro-indenoquinoxaline pyrrolidine or spiro-indenoquinoxaline pyrrolizidine systems, thus providing more opportunities for the development of a wide range of biologically active compounds. Hence, as a result of the aforementioned reasons and in continuation of our investigations towards the synthesis of various spiro heterocyclic compounds,[10] we herein report, a mild, expeditious, and facile four-component, one-pot synthesis of novel heterocyclic chiral spiro-indenoquinoxaline pyrrolidine and spiro-indenoquinoxaline pyrrolizidine systems with high regio-, diastereo- (>96:4 dr), and enantioselectivity (>99% ee) through a catalyst-free, one-pot, four-component 1,3-dipolar cycloaddition reaction of various amino acid, L-proline **4**, *trans*-4-hydroxy-L-proline **5** or sarcosine **6** with ninhydrin **1**,

* Corresponding author. Tel./fax: +98 021 22431661.
E-mail address: k-jadidi@sbu.ac.ir (K. Jadidi).

http://dx.doi.org/10.1016/j.tetasy.2015.08.013
0957-4166/© 2015 Elsevier Ltd. All rights reserved.

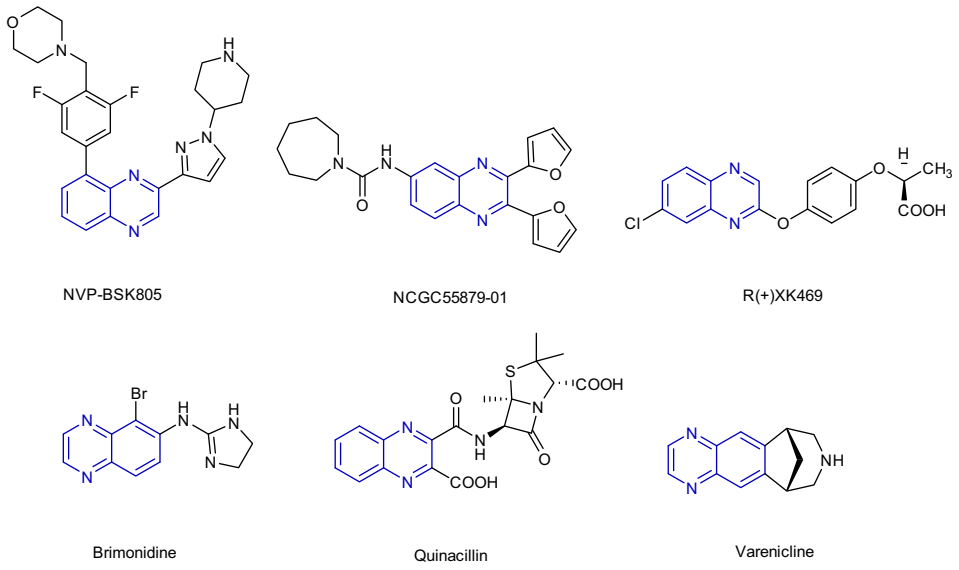

Figure 1. Some biologically important drugs and molecules with a quinoxaline moiety.

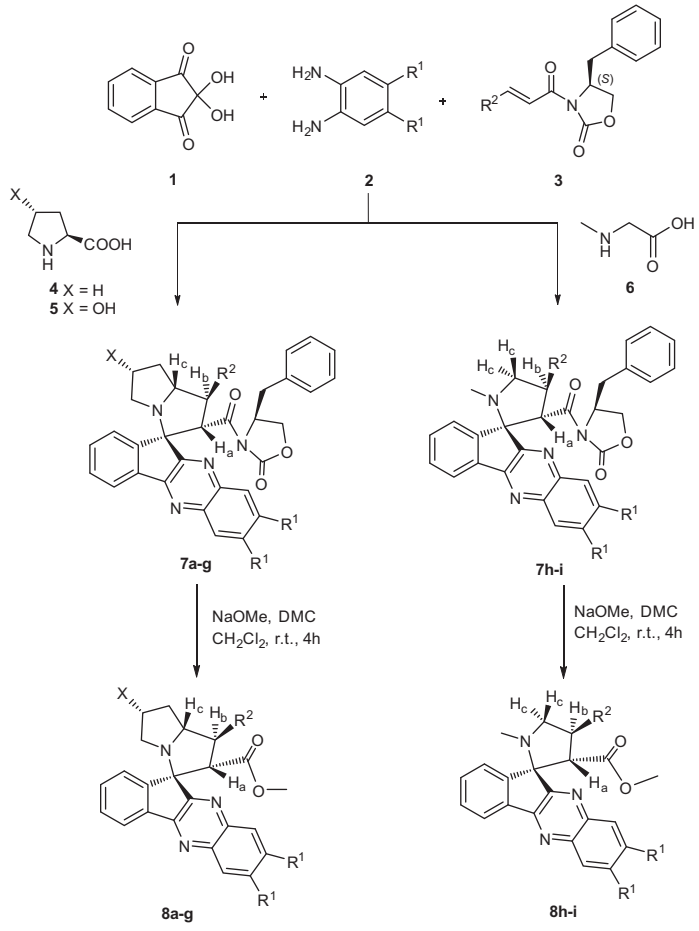

Scheme 1. Asymmetric synthesis of new chiral spiro-indenoquinoxaline pyrrolidine and spiro-indenoquinoxaline pyrrolizidine **7** and **8**.

phenylenediamines **2**, and optically active cinnamoyl–crotonoyl oxazolidinone **3** as mentioned in Scheme 1.

Over the past decade, the understanding of the selectivity behaviour in the polar [3+2] cycloaddition reactions has evolved from a successful interplay between theory and experiment. In this regard, a theoretical analysis of regio- and stereoselectivity of the 1,3-dipolar cycloaddition reaction of azomethine ylide **10** (Scheme 2) with cinnamoyl–crotonoyl oxazolidinone **3** was carried out by calculating the relevant transition states and reactivity indices.

Please cite this article in press as: Shahrestani, N.; et al. *Tetrahedron: Asymmetry* (2015), http://dx.doi.org/10.1016/j.tetasy.2015.08.013

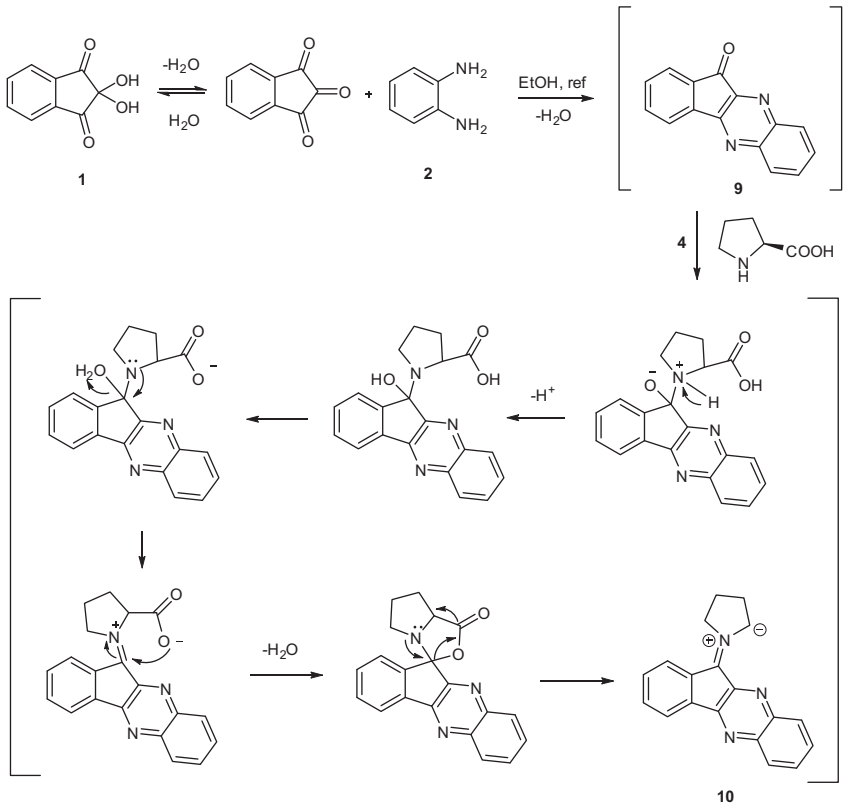

Scheme 2. Mechanism for the formation of azomethine ylide **10** from ninhydrin **1**, 1,2-phenylenediammine **2**, and L-proline **4**.

2. Result and discussion

Herein ninhydrin **1** and phenylenediamine **2** were condensed, and indenoquinoxaline **9** was formed. Next, after condensation of an amino acid (cyclic or linear) with **9** and decarboxylation of amino acid, non-stabilized azomethine ylide **10** was produced (Scheme 2). The [3+2] cycloaddition of chiral dipolarophile **3** with azomethine ylide **10** led to the formation of new chiral spiro-indenoquinoxaline pyrrolizidine **7**, which contains four contiguous stereogenic centres (Scheme 1). Despite the fact that sixteen different stereoisomers could be prepared theoretically, only diastereoisomer **7** was obtained in high yield and with high enantiomeric purity using this strategy. Finally, in order to explore the scope and generality of the present strategy, a small library of new chiral spiro-indenoquinoxaline pyrrolizidines and spiro-indenoquinoxaline pyrrolidines **7a–i** was synthesized and the results are summarized in Table 1.

The one-pot, four-component, 1,3-dipolar cycloaddition was carried out under mild conditions in aqueous ethanol and in the absence of any catalyst or Lewis acids.

Chiral cinnamoyl–crotonoyl oxazolidinone **3** was conveniently prepared from the corresponding acid chloride [usually obtained from the acid after treatment with $(COCl)_2$] and chiral oxazolidinone after deprotonation with a base such as NaH.[11]

Various chiral auxiliaries, such as camphorsultam and menthol, were screened in the reaction but in general no separable diastereomeric cycloadducts were obtained and the achieved diastereofacial selectivity was low to moderate.

The one-pot four component reaction was also carried out in toluene and acetonitrile and it was found that even under refluxing conditions, there was no improvement in the reaction results. This was attributed to the poor solubility of the reactant in toluene and acetonitrile, especially the amino acids.

The structures of the cycloadducts were assigned from their elemental and spectroscopic analyses including IR, ^{1}H NMR, ^{13}C NMR, and mass spectra data. Thus, the IR spectrum of spiro-indenoquinoxaline pyrrolizidine **7a** showed two strong peaks around 1779 and 1692 cm^{-1} indicating the presence of two carbonyl groups. The observation of two characteristic triplets and one doublet in the ^{1}H NMR spectra of compounds **7** and **8** unambiguously

Table 1
New chiral spiro-indenoquinoxaline pyrrolidines and spiro-indenoquinoxaline pyrrolidines **7** and **8**

Entry	Amino acid	R_1	R_2	Product	**7**		**8**	
					Yield (%)	$[\alpha]_D^{20c}$	Yield (%)	$[\alpha]_D^{20c}$
1	**4**	H	Ph	**a**	94	+165.3	98	−18
2	**4**	H	CH_3	**b**	96	+134.7	97	−17
3	**4**	CH_3	Ph	**c**	94	+164	97	−23.4
4	**4**	CH_3	CH_3	**d**	96	+136.7	95	−20.2
5	**5**	H	Ph	**e**	92	+112	83	−14
6	**5**	CH_3	Ph	**f**	92	+111.2	84	−18
7	**5**	H	CH_3	**g**	90	+128	83	−16.4
8	**6**	H	Ph	**h**	82	+270.7	96	−34
9	**6**	H	CH_3	**i**	81	+273.1	92	−33

Please cite this article in press as: Shahrestani, N.; et al. *Tetrahedron: Asymmetry* (2015), http://dx.doi.org/10.1016/j.tetasy.2015.08.013

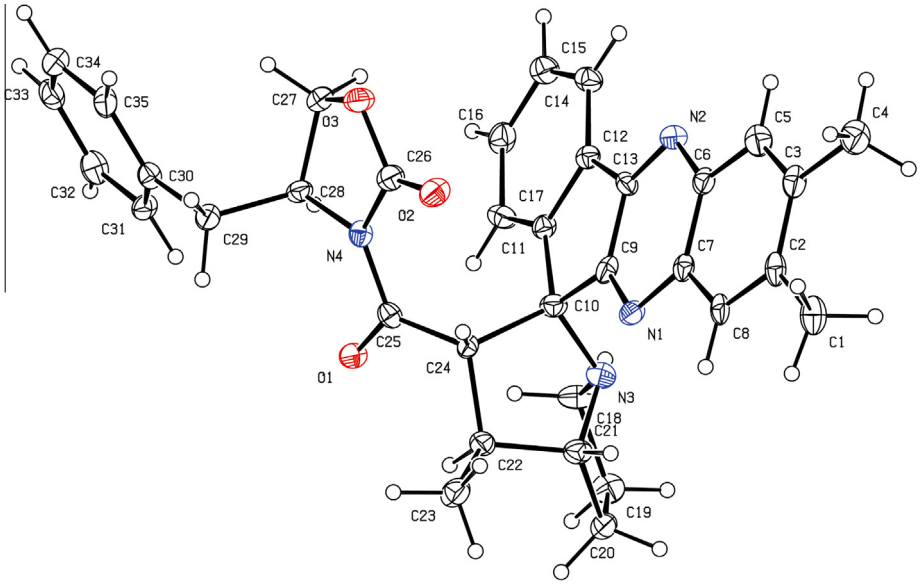

Figure 2. The ORTEP diagram of **7d**. Thermal ellipsoids are at 30% probability level.

confirmed the formation of a new pyrrolizidine ring. The pyrrolizidine ring proton attached to the phenyl ring appeared as a triplet at δ 4.32 (H_b). The pyrrolizidine NCH proton appeared as a multiplet at δ 4.98 (H_c), whereas the pyrrolizidine proton attached to the cinnamoyl oxazolidinone moiety was more deshielded and exhibited a doublet at δ 5.30 (H_a, J = 9 Hz). The aromatic protons appeared as a multiplet in the region δ 6.93–8.27. The off resonance decoupled ^{13}C NMR spectra of **7a** exhibited characteristic peaks for the spiro carbon at 73.2 ppm and carbonyls group attached to the cinnamoyl oxazolidinone moiety at 165.9 and 172.4 ppm; the signals for all other carbons were located at appropriate chemical shifts in agreement with the proposed structure.

The formation of the product was confirmed by mass spectra and elemental analyses. The mass spectrum of **7a** showed a peak at m/z 501 (M-91). The absolute configuration of chiral spiro-indenoquinoxaline pyrrolizidine **7d** was determined by single-crystal X-ray analysis as (3′*R*) (spiro carbon C10), (7a′*R*) (C21), (1*S*) (C22), (2*S*) (C24) (Fig. 2).[12,13]

Particularly noteworthy is the fact that all of the covalently attached azomethine ylide auxiliaries require destructive removal. It was in this context that we initiated studies where our goal was to develop a recoverable chiral auxiliary. For compounds **7a–i**, the chiral auxiliary was removed easily with sodium methoxide and dimethyl carbonate in CH_2Cl_2 and provided access to a variety of enantiomerically pure products **8a–i** in excellent to quantitative yields (Scheme 1). It should be noted that the auxiliary was recovered from this reaction in high yield.[14]

The stereochemistry and the structure of resulted cycloadduct **8a** were evaluated by using ^1H NMR and ^{13}C NMR and also 2D NMR spectroscopy techniques. The ^{13}C NMR spectrum displayed 29 signals, which were classified into 1 methyl, 3 methylene, 16 methines, and 9 quaternary carbons including a spiro carbon by the DEPT 135° experiments. In the HMQC spectrum of product **8a**, the positions of the three protons (H_a, H_b, and H_c) that were directly bonded to these carbon atoms (CH) were assigned. The ^1H NMR spectrum displayed two signals at δ = 3.898 and δ = 4.367 ppm (H_b, H_c respectively) and exhibited a doublet at δ 4.571 (H_a, J = 12 Hz); the H_b could be *trans* to H_c, because of the absence of any correlation between them in the ROESY spectrum. This was also confirmed from the weak NOE pattern between them. In order to determine the exact regioselectivity, the connectivity of the carbons in the molecular structure was obtained by using the analysis of the HMBC spectra. Based on the HMBC spectrum, there was no correlation between H_c and the signal of carbonyl group, which confirms the presence of a carbonyl group at C-2′ position in **8a** (instead of C-1′).

The formation of the product was confirmed by mass spectra and elemental analyses. The mass spectrum of **8a** showed a peak at m/z 448 (m+1).

It is known that chiral cinnamoyl–crotonoyl oxazolidinone, in the absence of Lewis acids, prefers a low energy *Z*-conformer of (*S*)-*cis*. The B3lyp/6-31G(d,p) calculations also show that *Z*-conformer of **3** is 9.2 Kcal/mol more stable than the *U*-conformer (Scheme 3). Thus, on the basis of the absolute configuration of the four stereogenic centres in the pyrrolizidine ring, it is assumed that the azomethine ylide approaches from the *endo*-*Si*-face of the dipolarophile as a *Z*-conformer of (*S*)-*cis* (Scheme 4).

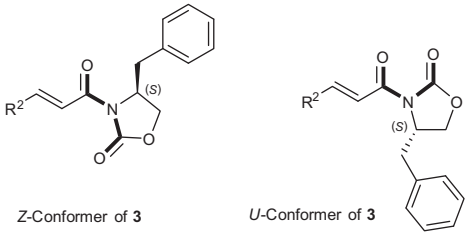

Scheme 3. *S-cis* conformations of **3**.

In recent years, 1,3-dipolar cycloaddition reactions have been the subject of several DFT studies showing that hybrid functionals such as B3LYP,[15] together with the standard 6-31G(d) and 6-31G(d,p) basis sets, produce satisfactory results.[16] Herein, the full geometrical optimization of all structures corresponding to potential energy minima and also related transition states (TSs) was carried out using this methodology. No symmetrical restriction was applied during geometrical optimizations. The nature of stationary geometries has been characterized by calculating the frequencies in order to verify that the transition states have only one imaginary frequency with the corresponding eigenvector involving the formation of the newly created C–C bonds. The electronic structures of the stationary points and transition structures were studied by the natural bond orbital (NBO) method.[17] Furthermore, harmonic frequencies, zero-point energies and thermodynamic corrections were obtained by using analytical force constants. Thermal

corrections to enthalpy and entropy values were evaluated at 298.15 K. All calculations were carried out with the Gaussian 09 suite of programs (Scheme 4).[18]

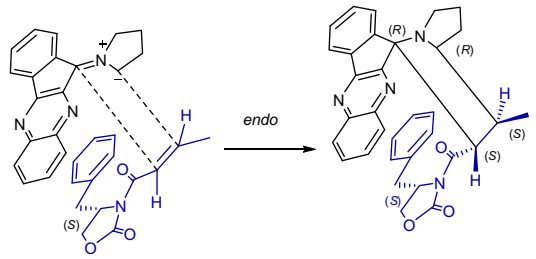

Scheme 4. Proposed models for *endo-Si*.

The analysis of gas-phase results indicated that the 1,3-dipolar cycloaddition reaction of dipole **11** with dipolarophile **3** take place along asynchronous concerted processes. The possible regio- and stereoisomeric pathways are shown in Scheme 5. Therefore four TSs, **TS 7d**, **TS 12**, **TS 13**, **TS 14** and their corresponding cycloadducts were located and characterized. The relative energies are compiled in Table 2 and Figure 4. The geometries of the TSs are presented in Figure 3.

As shown in Table 2, the activation barriers associated to these cycloadditions are: 6.5 kcal/mol for **TS 7d**, 10.3 kcal/mol for **TS 12**, 13.7 kcal/mol for **TS 13** and 14.5 kcal/mol for **TS 14**. Accordingly, it can be predicted that the **7d** regioisomer will be formed preferentially, which is in good agreement with the experimental observations. These cycloadditions are exothermic by approximately −18 to −22.6 kcal/mol. The calculated activation barriers for the *endo* approaches are lower than those for the *exo* approaches (Table 2 and Fig. 4).

The analysis of the geometries at the TSs is given in Figure 3 and indicates that this reaction takes place along asynchronous processes. In an asynchronous cycloaddition reaction, the approach of the reactants to each other and the new bonds formation in the TS are asymmetric processes. The synchronicity (Sy) index of the cycloaddition reactions is estimated by the equation[19]

$$Sy = 1 - (2n-2)^{-1}\sum_{i=1}^{n}\frac{|\delta B_i - \delta B_{av}|}{\delta B_{av}} \quad (1)$$

where n is the number of bonds directly involved in the reaction and δB_i is the relative variation of the Wiberg bond indices[20] for the bonds in the TS, which is calculated by the equation:

$$\delta B_i = \frac{B_i^{Ts} - B_i^{R}}{B_i^{P} - B_i^{R}} \quad (2)$$

Here, superscript indices P, R, and TS correspond to the product, reactant, and transition state. The average variation δB_{av}, in Eq. (1) is determined by:

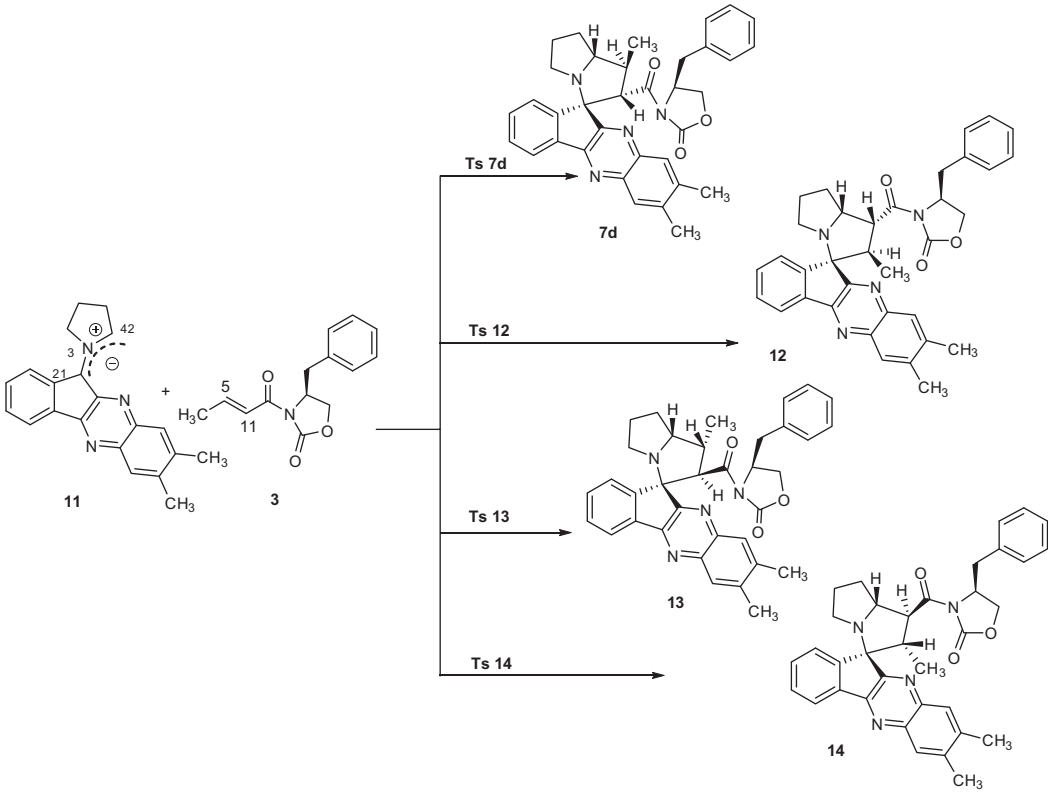

Scheme 5. Regio- and stereoisomeric pathways for a 1,3-dipolar cycloaddition reaction between azomethine ylide **11** with crotonoyl oxazolidinone **3**.

Table 2
Calculated electronic activation energies E_a, reaction Gibbs free energies ΔG, reaction enthalpies ΔH, reaction energies ΔE_{rxn}, activation Gibbs free energies $\Delta G^{\#}$, activation enthalpies $\Delta H^{\#}$ and Average Bond Index Changes (δB_{av}), Synchronicities (Sy) at B3lyp/6-31G(d,p), all energies are in kcal/mol

Structure	ΔE_{rxn}	ΔH	ΔG	E_a	$\Delta H^{\#}$	$\Delta G^{\#}$	ΔR	Sy	δB_{av}
7d	−19.7	−19.9	−4.9	6.5	6.8	21.0	0.701	0.46	0.25
12	−21.3	−21.6	−6.4	10.3	10.5	24.8	0.489	0.69	0.35
13	−18.0	−18.2	−3.1	13.7	14.2	27.0	0.808	0.22	0.23
14	−22.6	−22.8	−8.0	14.5	14.7	28.9	0.045	0.85	0.38

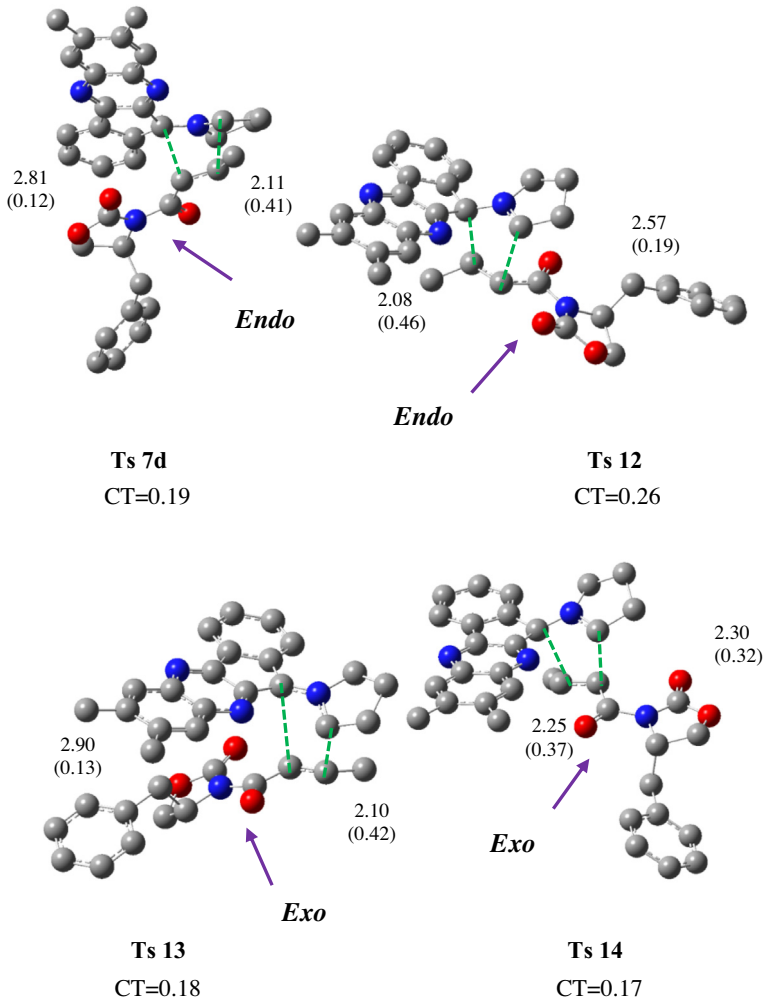

Figure 3. Transition structures corresponding to the regioisomeric and stereoisomeric pathways of the 1,3-dipolar cycloaddition reaction channels. The bond lengths directly involved in the reaction are given in angstroms. The bond orders are given in parenthesis. Hydrogen atoms have been omitted for the sake of clarity. The charge transfers (CT) are given in a.u.

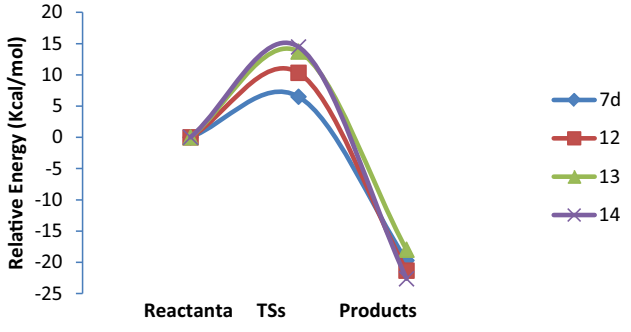

Figure 4. Relative energies (kcal/mol) for the reactants, TSs and products for the four possible reaction channels.

$$\delta B_{av} = n^{-1}\sum_{i=1}^{n}\delta B_i \quad (3)$$

According to Eq. (1), for a perfectly synchronous process, $Sy = 1$ and for a fully asynchronous process synchronicity is zero. Based on Eqs. (2) and (3), early and late transition structures will be characterized by $\delta B_{av} < 0.5$ and $\delta B_{av} > 0.5$, respectively.[19g] Wiberg bond indices for reactants, transition structures and products are shown in Table 3.

Table 3
Wiberg bond indices for reactants, transition structures and products indicated in Scheme 5

Structure	$B_{2,1,3}$	$B_{3,4,2}$	$B_{5,1,1}$	$B_{5,4,2}$	$B_{5,2,1}$	$B_{11,4,2}$	$B_{11,2,1}$
3	–	–	1.82	–	–	–	–
11	1.13	1.42	–	–	–	–	–
Ts 7d	1.16	1.21	1.46	0.41	–	–	0.12
Ts 12	1.05	1.38	1.36	–	0.46	0.19	
Ts 13	1.20	1.19	1.44	0.42	–	–	0.13
Ts 14	1.08	1.29	1.38	–	0.37	0.32	–
7d	0.97	0.95	0.98	0.97	–	–	0.91
12	0.95	0.96	0.98	–	0.95	0.94	–
13	0.96	0.95	0.97	0.97	–	–	0.93
14	0.97	0.95	0.97	–	0.94	0.96	–

The extent of the asynchronicity of the bond formation in a cycloaddition reaction can also be measured through the difference between the lengths of the two σ bonds that are being formed in the reaction. The computed synchronicities (Sy) and the ΔRs for the four possible channels in Table 2 show that the asynchronicities order is **Ts 13** > **Ts 7d** > **Ts 12** > **Ts 14** which complies with the stability of the products. The $\delta B_{av}s$ are in all cases indicative of an early transition state which is in agreement with the exothermic nature of the reactions (Table 2).

Table 4
Calculated global properties of dipole **6** and dipolarophile **3** at B3lyp/6-31G(d,p)

Structure	ε_{HOMO} (eV)	ε_{LUMO} (eV)	ω (eV)	μ (a.u.)	η (a.u.)	S (a.u.)	N
Azomethine ylide **11**	−4.44	−1.39	1.40	−0.1071	0.112	4.478	4.68
Cinnamoyl–crotonyl oxazolidinone **3**	−6.75	−1.36	1.53	−0.1492	0.198	2.524	2.37

Recent studies have shown that the defined global and local indices in the context of density functional theory are powerful tools for helping understand the behaviour of 1,3-DC reactions.[21] The charge transfer ability of a molecule in its ground state can be described by the electronic chemical potential, which is defined as the arithmetic mean of one-electron energies of the frontier molecular orbital HOMO and LUMO, ε_H and ε_L as $\mu = (\varepsilon_H + \varepsilon_L)/2$. The chemical hardness η, which is a measure of the stability of a system, may be approached in terms of ε_H and ε_L as $\eta = \varepsilon_L - \varepsilon_H$.[22] The global electrophilicity index ω, which measures the stabilization in energy when the system acquires an additional electronic charge ΔN from the environment, was given the following simple expression, $\omega = (\mu^2/2\eta)$,[22] in terms of the electronic chemical potential and the chemical hardness. On the other hand, the nucleophilicity index for a given system was defined as $N = \varepsilon_{HOMO} - \varepsilon_{HOMO\ (TCE)}$, where ε_{HOMO} is the HOMO energy of the nucleophile and $\varepsilon_{HOMO\ (TCE)}$ corresponds to the HOMO energy of the tetracyanoethylene (TCE) taken as a reference.[23]

The calculated global properties μ, η, ω and N are shown in Table 4. The electrophilicity (ω) of **3** is greater than 1.5 eV, so it could be classified as a strong electrophile within the electrophilicity scale[24a] while the azomethine ylide has a large nucleophilicity value, $N = 4.68$ eV. The electronic chemical potential, μ and the nucleophilicity index, N of the azomethine ylide **11** is higher than the cinnamoyl–crotonoyl oxazolidinone **3** while the electrophilicity of **3** is greater than the **11**; therefore during a polar process a net charge transfer will take place from the azomethine ylide to the alkene, which is in agreement with the charge transfer found at the TSs. As shown in Figure 5, the energy gap between $HOMO_{13}$ and $LUMO_3$ (3.074 eV) is lower than the $LUMO_{13}$ and the $HOMO_3$ (5.360 eV). This attests that the HOMO–LUMO energy gaps (Table 4) also suggest that the $HOMO_{dipole}$–$LUMO_{dipolarophile}$ interaction controls the cycloaddition reactions (normal electron demand reactions).[25]

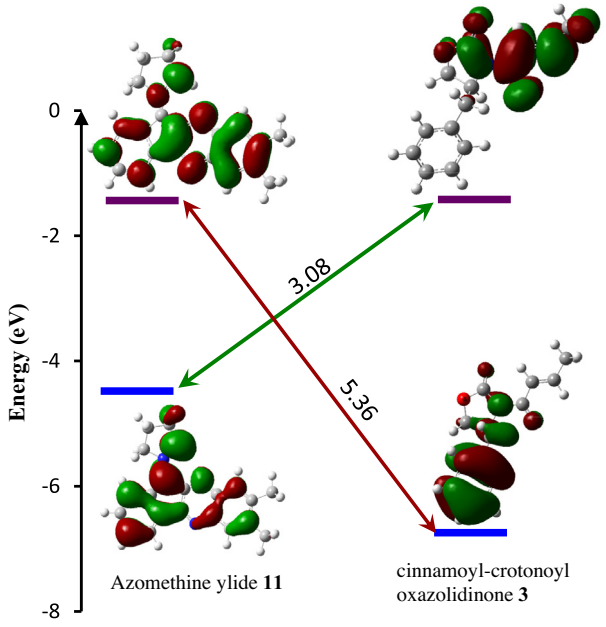

Figure 5. The HOMO–LUMO energy gaps.

The DFT-based reactivity indices such as Fukui functions and local electrophilicity indices were evaluated on the dipole and dipolarophile reagents with the aim of describing the experimentally observed regioselectivity.[24c–g] We calculated a Fukui function for nucleophilic (f_k^+) and electrophilic (f_k^-) attacks through the Mulliken charges analysis using Eqs. (4) and (5), respectively[24h]

$$f_k^+ = \rho_k^{N+1} - \rho_k^N = q_k^N - q_k^{N+1} \quad (4)$$

$$f_k^- = \rho_k^N - \rho_k^{N-1} = q_k^{N-1} - q_k^N \quad (5)$$

with k, N, ρ and q, corresponding to the index of the atom, the number of electrons, the population number and the net charge stemming from calculations, respectively.

The local electrophilicity index, ω_k, can be measured by $\omega_k = \omega f_k^+$.[24] This expression shows that wherever f_k^+ has its maximum value, i.e. at the active site of the electrophile. For polar cycloaddition reactions the most favourable regioisomeric pathway corresponds to the bond-formation at the most electrophilic and nucleophilic sites of the unsymmetrical reactants. Therefore, the regioselectivity of these cycloaddition reactions can be explained by using the local electrophilicity index ω_k, at the more electrophile reactant together with the nucleophilic Fukui functions, f_k^-, at the less electrophilic one. In Table 5, the electrophilic, f_k^+ and nucleophilic, f_k^-, Fukui functions and local electrophilicities contributions to the respective atomic centres are summarized.

Cinnamoyl–crotonoyl oxazolidinone **3** has the largest electrophilic activation at the C5 carbon atom, $\omega_k = 0.108$ eV, whereas the azomethine ylide **11** has the largest nucleophilic activation at the C42 carbon atom, $f_k^- = 0.120$ (see Table 5). Therefore, C5 of cinnamoyl–crotonoyl oxazolidinone **3** will be the preferred position for a nucleophilic attack by C42 of the azomethine ylide **11**, which is in good agreement with the experimental observations.

The regioselectivity in the cycloaddition reactions has also been described in terms of a local hard and soft acid and bases principle, formulated with density functional theory (DFT).[26] The HSAB principle indicates that the interaction between A and B is favored when it occurs through those atoms with approximately equal softness values. According to chemical potentials and electrophilicity indices, as well as the HOMO–LUMO energy gaps, dipoles and dipolarophiles are classified as nucleophiles or electrophiles. When

Table 5
Calculated local properties of dipole **13** and dipolarophile **3** at B3lyp/6-31G(d,p)

Reactant	Site	f_k^+	f_k^-	ω_k(eV)	s^+	s^-
3	C5	0.071	0.032	0.108	0.179	0.081
3	C11	0.020	0.027	0.030	0.050	0.068
11	C21	0.025	0.092	0.034	0.112	0.414
11	C42	0.028	0.120	0.039	0.125	0.538

atoms *i* and *j* of a molecule A (nucleophile) are involved in the formation of a cycloadduct with atoms *k* and *i* of another molecule B (electrophile), Δ can be considered as a measure of predominance of one approach over the other. The reaction path associated with the lower Δ value will be the preferred one.

$$\Delta_{ij}^{kl} = (s_i^- - s_k^+)^2 + (s_j^- - s_l^+)^2 \quad (6)$$

where s_is are the appropriate type of atomic softness and they calculated as

$$s_k^{\pm} = f_k^{\pm} S \quad (7)$$

where S is the global softness and computed as[27]

$$S = \frac{1}{2\eta} \quad (8)$$

Herein, cinnamoyl–crotonoyl oxazolidinone **3** behaves as an electrophile and azomethine ylide **11** as a nucleophile. The calculated Δ_{ij}^{kl} values for the generation of **7d** (0.261) is smaller compared to that for the generation of **12** (0.293) (Table 3). This observation is in good agreement with the experimental observation.

3. Conclusion

In conclusion, we have prepared a small library of new chiral spiro-indenoquinoxaline pyrrolidines and chiral spiro-indenoquinoxaline pyrrolizidines through a one-pot, four-component reaction between ninhydrin, *o*-phenylenediamine derivatives, amino acid, and chiral cinnamoyl–crotonoyl oxazolidinone under mild reaction conditions in the presence of environmentally friendly aqueous ethanol as the solvent. The products were obtained in excellent yields (up to 96%) and with excellent enantiomeric purity (up to 99%). The removal of the chiral auxiliary was easily achieved without racemization or by-product formation. The regiochemistry of the cycloaddition has been explained successfully by using the density functional theory based on global and local reactivity indices and HSAB principle as well as the analysis of the activation energies.

4. Experimental

4.1. General

Melting points were measured by an Electrothermal 9200 apparatus. IR spectra were recorded on FT-IR 102 MB BOMEM apparatus. ^{1}H and ^{13}C, DEPT 135, ROSEY, HMQC and HMBC spectra were determined on a BRUKER DRX-300 AVANCE spectrometer at 300.13 and 75.47 MHz, respectively. MS spectra were recorded on a Shimadzu QP 1100EX mass spectrometer operating at an ionization potential of 70 eV.

4.2. Typical procedure for the preparation of (*S*)-4-benzyl-3-((1′*R*,2′*S*,3′*R*,7a′*R*)-1′-phenyl-1′,2′,5′,6′,7′,7a′-hexahydrospiro-[indeno-[1,2-*b*]quinoxaline-11,3′-pyrrolizine]-2′-ylcarbonyl)-oxazolidin-2-one 7a

A mixture of ninhydrin **1a** (0.178 g, 1 mmol) and 1,2-phenylenediamine **2a** (0.108 g, 1 mmol) was stirred for 10 min in ethanol (10 mL). To this solution were added amino acid **4** (0.115 g, 1 mmol) and cinnamoyl oxazolidinone **4a** (0.307 g, 1 mmol), after which it was heated at reflux for approximately 20 h (the progress of the reaction was monitored by TLC). The solvent was removed under reduced pressure and the crude product was purified by column chromatography using n-hexane/ethyl acetate (70:30) as eluent to afford pure **7a** in 94% yield.

4.3. Typical procedure for the preparation of (1′*R*,2′*S*,3′*R*,7a′*R*)-methyl1′-phenyl-1′,2′,5′,6′,7′,7a′-hexahydrospiro[indeno[1,2-*b*]-quinoxaline-11,3′-pyrrolizine]-2′-carboxylate 8a

To a solution of **7a** (609 mg, 1.03 mmol) in CH_2Cl_2 (5 mL), were added sodium methoxide (275 mg, 5.15 mmol), and dimethyl carbonate (0.42 mL, 5.15 mmol) after which it was stirred at room temperature for 4 h (the reaction time for *trans*-4-hydroxy-L-proline derivatives was 6 h). After the reaction was complete, water (5 mL) was added and the organic layer was separated. The aqueous layer was acidified to ca. pH 7 with hydrochloric acid and extracted with CH_2Cl_2. The combined organic layer was dried over $MgSO_4$, filtered, and concentrated in vacuo. The mixture was chromatographed on silica gel by ether–hexane (1/2) to afford pure **8a** in 98% yield and (*S*)-4-benzyloxazolidin-2-one in 96% yield.

4.4. (*S*)-4-Benzyl-3-((1′*R*,2′*S*,3′*R*,7a′*R*)-1′-phenyl-1′,2′,5′,6′,7′,7a′-hexahydrospiro[indeno[1,2-*b*]quinoxaline-11,3′-pyrrolizine]-2′-ylcarbonyl)oxazolidin-2-one 7a

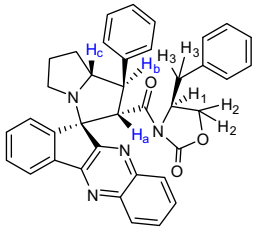

Yellow oily liquid (550 mg, 94%); IR (KBr) (ν_{max}/cm^{-1}): CO 1779, 1692; ^{1}H NMR (300 MHz, $CDCl_3$): δ_H (ppm) = 1.60–1.70 (m, 1H, pyrrolizine), 1.90–1.99 (m, 2H, pyrrolizine), 2.04–2.15 (m, 2H, pyrrolizine), 2.54–2.61 (dd, 1H, J = 13.35, 9 Hz, H_3), 2.63–2.68 (m, 1H, pyrrolizine), 2.94–2.99 (dd, 1H, J = 13.5, 2.7 Hz, H_3), 3.25–3.40 (m, 1H, H_2), 3.71–3.75 (dd, 1H, H_2), 4.17–4.25 (m, 1H, H_1), 4.28–4.36 (m, 1H, H_b), 4.95–5.00 (m, 1H, H_c), 5.30 (d, 1H, J = 9 Hz, H_a), 6.93–8.27 (m, 18H, Arom); ^{13}C NMR (75 MHz, $CDCl_3$): δ_c (ppm) = 25.3, 27.4, 37.5, 48.5, 52.9, 55.4, 62.7, 65.6, 71.8, 73.2, 122.7, 126.7, 126.9, 128.7, 128.9, 129.1, 129.2, 129.2, 129.7, 129.9, 130.1, 134.8, 139.0, 140.9, 141.8, 142.4, 143.8, 151.9, 152.0, 165.9, 172.4; MS *m*/*z* (%): 501 (M-91) (%48), 434 (%75), 386 (%38), 319 (%56), 218 (%50), 131 (%80); $[\alpha]_D^{20}$ = +165.3 (*c* 0.03, CH_2Cl_2).

4.5. (*S*)-4-Benzyl-3-((1′*S*,2′*S*,3′*R*,7a′*R*)-1′-methyl-1′,2′,5′,6′,7′,7a′-hexahydrospiro[indeno[1,2-*b*]quinoxaline-11,3′-pyrrolizine]-2′-ylcarbonyl)oxazolidin-2-one 7b

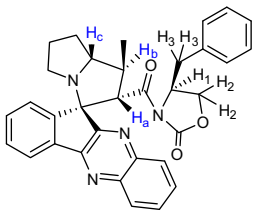

Yellow solid (508 mg, 96%); IR (KBr) (ν_{max}/cm^{-1}): CO 1779, 1686; ^{1}H NMR (300 MHz, $CDCl_3$): δ_H (ppm) = 1.36 (d, 3H, J = 6.6 Hz, CH_3), 1.87–2.21 (m, 5H, pyrrolizine), 2.57–2.60 (m, 1H, pyrrolizine),

2.60–2.64 (dd, 1H, H_3), 3.03–3.12 (dd, 1H, H_3), 3.03–3.12 (m, 1H, H_2), 3.23–3.28 (m, 1H, H_1), 3.72–3.75 (m, 1H, H_2), 4.03 (m, 1H, H_b), 4.33 (m, 1H, H_c), 4.82 (d, 1H, J = 9.6 Hz, H_a), 7.08–8.20 (m, 13H, Ar); ^{13}C NMR (75 MHz, $CDCl_3$): δ_c (ppm) = 16.1, 26.0, 28.2, 37.8, 41.4, 48.2, 55.9, 61.4, 65.7, 70.8, 73.8, 122.4, 127.7, 127.2, 128.7, 128.8, 129.0, 129.3, 129.9, 130.1, 135.2, 138.6, 142.0, 142.4, 144.2, 151.9, 165.5, 172.5; MS *m*/*z* (%): 530(M) (%62), 501 (%38), 434 (%70), 353 (%45), 326 (%78), 218 (%78), 97 (%80); $[\alpha]_D^{20}$ = +134.7 (*c* 0.03, CH_2Cl_2).

4.6. (*S*)-4-Benzyl-3-((1′*R*,2′*S*,3′*R*,7a′*R*)-7,8-dimethyl-1′-phenyl-1′,2′,5′,6′,7′,7a′-hexahydrospiro[indeno[1,2-*b*]quinoxaline-11,3′-pyrrolizine]-2′-ylcarbonyl)oxazolidin-2-one 7c

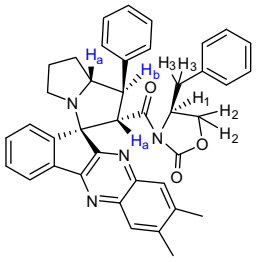

Yellow oily liquid (580 mg, 94%); IR (KBr) (ν_{max}/cm^{-1}): CO 1781, 1689; ^{1}H NMR (300 MHz, $CDCl_3$): δ_H (ppm) = 1.88–2.01 (m, 2H, pyrrolizine), 2.05–2.19 (m, 3H, pyrrolizine), 2.25–2.55 (d, 6H, $2CH_3$), 2.61–2.70 (dd, 1H, H_3), 2.93–2.99 (dd, 1H, H_3), 3.23–3.31 (m, 1H, H_2), 3.69–3.73 (dd, 1H, H_2), 4.11–4.26 (m, 1H, H_1), 4.24–4.31 (m, 1H, H_b), 4.93–4.99 (m, 1H, H_c), 5.30 (d, 1H, J = 9.3 Hz, H_a), 6.93–8.27 (m, 16H, Ar); ^{13}C NMR (75 MHz, $CDCl_3$): δ_c (ppm) = 20.2, 20.2, 25.4, 27.4, 37.5, 48.5, 52.8, 55.5, 62.7, 65.6, 71.7, 73.4, 122.7, 126.7, 126.9, 128.7, 128.9, 129.1, 129.2, 129.2, 129.7, 129.8, 134.9, 139.1, 139.2, 139.4, 140.7, 140.9, 141.1, 143.8, 151.9, 151.9, 165.9, 172.4; MS *m*/*z* (%): 620 (M) (%35), 444 (%63), 416 (%70), 245 (%42), 91 (%75); $[\alpha]_D^{20}$ = +164 (*c* 0.03, CH_2Cl_2).

4.7. (*S*)-4-Benzyl-3-((1′*S*,2′*S*,3′*R*,7a′*R*)-1′,7,8-trimethyl-1′,2′,5′,6′,7′,7a′-hexahydrospiro[indeno[1,2-*b*]quinoxaline-11,3′-pyrrolizine]-2′-ylcarbonyl)oxazolidin-2-one 7d

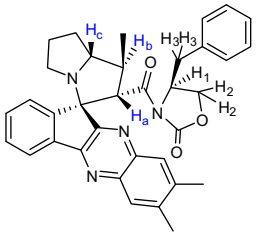

Yellow solid (533 mg, 96%); IR (KBr) (ν_{max}/cm^{-1}): CO 1780, 1688; ^{1}H NMR (300 MHz, $CDCl_3$): δ_H (ppm) = 1.35 (d, 3H, J = 6.3 Hz, 3H), 1.82–2.19 (m, 5H, pyrrolizine), 2.48–2.52 (d, 6H, $2CH_3$), 2.52–2.55 (m, 1H, pyrrolizine), 2.55–2.63 (dd, 1H, H_3), 2.98–3.10 (m, 2H, H_2, H_3), 3.23–3.28 (m, 1H, H_1), 3.70–3.73 (dd, 1H, H_2), 3.93 (m, 1H, H_b), 4.28 (m, 1H, H_c), 4.84 (d, 1H, J = 9.6 Hz, H_a), 7.06–8.16 (m, 13H, Ar); ^{13}C NMR (75 MHz, $CDCl_3$): δ_c (ppm) = 16.1, 20.2, 20.2, 28.7, 29.8, 38.0, 42.3, 49.2, 55.5, 59.4, 65.7, 69.7, 121.4, 123.8, 125.2, 127.7, 127.8, 128.9, 128.1, 129.9, 130.0, 130.0, 131.9, 135.4, 136.9, 141.8, 152.2, 164.8, 172.4; MS *m*/*z* (%): 558(M) (%28), 462 (%75), 382 (%20), 246(%60), 69 (%81); $[\alpha]_D^{20}$ = +136.7 (*c* 0.03, CH_2Cl_2).

4.8. (*S*)-4-Benzyl-3-((1′*R*,2′*S*,3′*R*,6′*R*,7a′*R*)-6′-hydroxy-1′-phenyl-1′,2′,5′,6′,7′,7a′-hexahydrospiro[indeno[1,2-*b*]quinoxaline-11,3′-pyrrolizine]-2′-ylcarbonyl)oxazolidin-2-one 7e

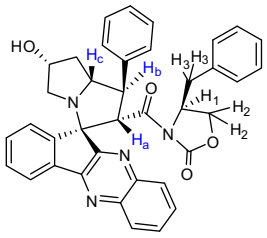

Yellow oily liquid (557 mg, 92%); IR (KBr) (ν_{max}/cm^{-1}): CO 1780, 1688, OH 3423; ^{1}H NMR (300 MHz, $CDCl_3$): δ_H (ppm) = 1.65–1.97 (m, 3H, pyrrolizine), 2.45–2.52 (m, 1H, pyrrolizine), 2.54–2.61 (dd, 1H, J = 13.05, 9.3 Hz, H_3), 2.72–2.77 (m, 1H, H_3), 2.95–3.03 (m, 1H, H_2), 3.21–3.27 (m, 1H, H′), 3.71–3.74 (m, 1H, H_2), 4.13–4.16 (m, 1H, H_1), 4.44 (m, 1H, OH), 4.47–4.50 (dd, 1H, H_b), 4.76–4.82 (m, 1H, H_c), 5.28 (d, 1H, J = 9 Hz, H_a), 6.93–8.24 (m, 18H, Ar); ^{13}C NMR (75 MHz, $CDCl_3$): δ_c (ppm) = 37.4, 38.1, 52.6, 55.3, 55.4, 63.2, 65.7, 70.8, 71.9, 73.7, 117.6, 119.8, 127.0, 127.2, 128.7, 128.8, 128.9, 129.1, 129.3, 129.3, 129.8, 130.5, 133.7, 134.8, 137.0, 138.5, 140.5, 141.6, 142.2, 143.9, 152.0, 152.2, 161.6, 165.4, 171.8; MS *m*/*z* (%): 608 (M) (32%), 524 (50%), 447 (42%), 404 (65%), 217 (60%), 91 (45%), 77; $[\alpha]_D^{20}$ = +112 (*c* 0.03, CH_2Cl_2).

4.9. (*S*)-4-Benzyl-3-((1′*R*,2′*S*,3′*R*,6′*R*,7a′*R*)-6′-hydroxy-7,8-dimethyl-1′-phenyl-1′,2′,5′,6′,7′,7a′-hexahydrospiro[indeno[1,2-*b*]quinoxaline-11,3′-pyrrolizine]-2′-ylcarbonyl)oxazolidin-2-one 7f

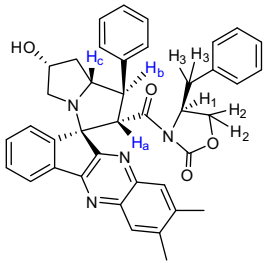

Yellow solid (580 mg, 92%); IR (KBr) (ν_{max}/cm^{-1}): CO 1781, 1689, OH 3424; ^{1}H NMR (300 MHz, $CDCl_3$): δ_H (ppm) = 1.65–1.93 (m, 4H, pyrrolizine), 2.50–2.53 (d, 6H, $2CH_3$), 2.71–2.76 (dd, 1H, J = 8.7, 6 Hz, H_3), 2.94–2.96 (m, 1H, H_3), 2.97–2.99 (m, 1H, H_2), 3.18–3.24 (m, 1H, H′), 3.68–3.72 (m, 1H, H_2), 4.07–4.12 (m, 1H, H_1), 4.40–4.47 (dd, 1H, H_b), 4.49–4.52 (m, 1H, OH), 4.73–4.81 (m, 1H, H_c), 5.30 (d, 1H, J = 9 Hz, H_a), 6.92–8.17 (m, 16H, Ar); ^{13}C NMR (75 MHz, $CDCl_3$): δ_c (ppm) = 20.2, 20.2, 37.4, 38.2, 52.5, 55.1, 55.5, 63.2, 65.6, 70.8, 71.8, 73.9, 122.2, 126.5, 127.0, 127.1, 128.4, 128.7, 128.7, 129.1, 129.2, 129.7, 130.0, 134.9, 138.7, 139.2, 139.5, 140.5, 140.5, 140.9, 143.7, 151.2, 151.8, 164.4, 171.8; MS *m*/*z* (%): 636 (M) (40%), 475 (55%), 433 (40%), 356 (23%), 158 (75%), 77 (43%); $[\alpha]_D^{20}$ = +111.2 (*c* 0.03, CH_2Cl_2).

4.10. (*S*)-4-Benzyl-3-((1′*S*,2′*S*,3′*R*,6′*R*,7a′*R*)-6′-hydroxy-1′-methyl-1′,2′,5′,6′,7′,7a′-hexahydrospiro[indeno[1,2-*b*]quinoxaline-11,3′-pyrrolizine]-2′-ylcarbonyl)oxazolidin-2-one 7g

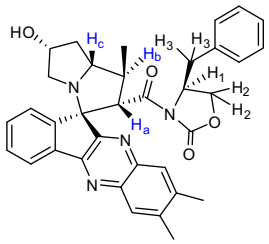

Yellow solid (490 mg, 90%); IR (KBr) (ν_{max}/cm^{-1}): CO 1779, 1673, OH 3423; ^{1}H NMR (300 MHz, $CDCl_3$): δ_H (ppm) = 1.34 (d, 3H, J = 9.6 Hz, CH_3), 1.68–1.76 (m, 1H, pyrrolizine), 2.18–2.57 (m, 3H, pyrrolizine), 2.60–2.63 (dd, 1H, H_3), 2.79–2.84 (dd, 1H, H_3), 3.07–3.12 (m, 1H, H_2), 3.18–3.24 (m, 1H, H′), 3.287–3.33 (m, 1H, OH), 3.72–3.75 (m, 1H, H_2), 4.03 (m,1H, H_1), 4.15–4.21 (dd, 1H, H_b), 4.49–4.53 (m, 1H, H_c), 4.79 (d, 1H, J = 9.3 Hz, H_a), 7.02–8.18 (m, 13H, Ar); ^{13}C NMR (75 MHz, $CDCl_3$): δ_c (ppm) = 16.1, 37.7, 38.5, 41.3, 54.9, 55.8, 62.1, 65.8, 69.8, 72.1, 74.2, 122.3, 126.7, 127.2, 128.8, 129.0, 129.2, 129.3, 129.7, 129.8, 130.4, 135.1, 138.3, 141.7, 142.2, 144.2, 152.0, 165.0, 171.9; MS m/z (%): 546(M) (35%), 455 (66%), 344 (25%), 217 (48%), 91 (80%); $[\alpha]_D^{20}$ = +128 (c 0.03, CH_2Cl_2).

4.11. (*S*)-4-Benzyl-3-((2′*R*,3′*S*,4′*R*)-1′-methyl-4′-phenylspiro-[indeno[1,2-*b*]quinoxaline-11,2′-pyrrolidine]-3′-ylcarbonyl)-oxazolidin-2-one 7h

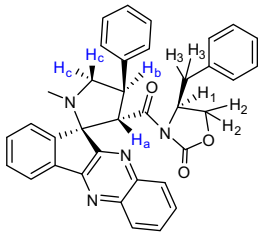

Yellow oily liquid (464 mg, 82%); IR (KBr) (ν_{max}/cm^{-1}): CO 1784, 1686; ^{1}H NMR (300 MHz, $CDCl_3$): δ_H (ppm) = 1.95 (S, 3H), 2.52–2.60 (dd, 1H, J = 13.5, 9.3 Hz, H_3), 2.97–3.03 (dd, 1H, J = 13.8, 2.7 Hz, H_3), 3.12–3.17 (m, 1H, H_c), 3.60–3.65 (m, 1H, H_c), 3.22–3.75 (dd, 1H, H_2), 4.06–4.11 (m, 1H, H_1), 4.14–4.209 (dd, 1H, H_2), 4.72–4.80 (dd, 1H, H_b), 5.03 (d, 1H, J = 8.7 Hz, H_a), 6.84–8.21 (m, 18H, Ar); ^{13}C NMR (75 MHz, $CDCl_3$): δ_c (ppm) = 34.2, 37.4, 45.0, 55.5, 60.5, 61.9, 65.7, 74.1, 122.1, 125.7, 126.9, 127.1, 127.8, 128.6, 128.7, 128.8, 128.9, 129.3, 129.6, 129.9, 131.0, 134.9, 138.4, 141.4, 141.6, 142.1, 145.9, 152.1, 153.0, 165.1, 171.3; MS m/z (%): 434 (M-132) (75%), 362 (20%), 317 (33%), 217 (15%), 133 (85%), 91 (42%); $[\alpha]_D^{20}$ = +270.7 (c 0.03, CH_2Cl_2).

4.12. (*S*)-4-Benzyl-3-((2′R,3′S,4′S)-1′,4′-dimethylspiro[indeno-[1,2-*b*]quinoxaline-11,2′-pyrrolidine]-3′-ylcarbonyl)oxazolidin-2-one 7i

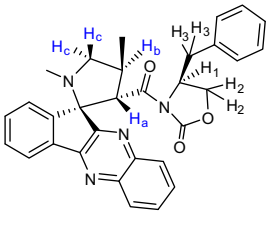

Yellow oily liquid (408 mg, 81%); IR (KBr) (ν_{max}/cm^{-1}): CO 1785, 1686; ^{1}H NMR (300 MHz, $CDCl_3$): δ_H (ppm) = 1.40 (d, 3H, J = 4.5 Hz), 1.87 (S, 3H), 2.57–2.64 (dd, 1H, H_3), 3.10–3.13 (m, 1H, H_3), 3.10–3.13 (m, 1H, H_2), 3.43–3.47 (m, 1H, H_c), 3.50–3.59 (m, 1H, H_c), 3.50–3.59 (m, 1H, H_1), 3.72–3.75 (m, 1H, H_2), 4.06 (m, 1H, H_b), 4.51 (d, 1H, J = 5.7 Hz, H_a), 7.10–8.14 (m, 18H, Ar); ^{13}C NMR (75 MHz, $CDCl_3$): δ_c (ppm) = 16.9, 35.2, 36.8, 38.3, 55.5, 59.1, 60.2, 65.7, 120.3, 121.7, 125.5, 127.2, 128.8, 128.6, 128.7, 129.8, 129.9, 130.3, 131.6, 135.9, 138.1, 142.6, 152.3, 165.1, 171.3; MS m/z: 504 (M) (24%), 257 (25%), 217 (20%), 91 (32%); $[\alpha]_D^{20}$ = +283.1 (c 0.03, CH_2Cl_2).

4.13. Methyl (1′*R*,2′*S*,7a′*R*,11*R*)-1′-phenyl-1′,2′,5′,6′,7′,7a′-hexahydrospiro[indeno[1,2-*b*]quinoxaline-11,3′-pyrrolizine]-2′-carboxylate 8a

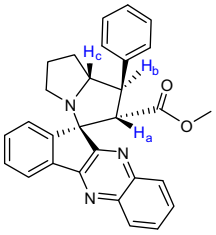

Yellow solid (438 mg, 98%); IR (KBr) (ν_{max}/cm^{-1}): CO 1721; ^{1}H NMR (300 MHz, $CDCl_3$): δ_H (ppm) = 1.73–2.18 (m, 4H, pyrrolizine), 2.52–2.66 (m, 2H, pyrrolizine), 2.85 (S, 3H, OCH_3), 3.86–3.93 (dd, 1H, H_b), 4.32–4.40 (m, 1H, H_c), 4.57 (d, 1H, J = 12 Hz, H_a), 7.27–8.34 (m, 13H, Arom); ^{13}C NMR (75 MHz, $CDCl_3$): δ_c (ppm) = 28.1, 30.9, 31.6, 47.8, 51.1, 52.8, 73.2, 75.2, 122.3, 127.0, 127.0, 128.0, 128.6, 128.7, 129.0, 129.4, 129.7, 129.9, 130.9, 138.1, 139.9, 142.4, 142.8, 144.1, 153.1, 170.0; MS m/z (%): 448 (M + 1) (24%), 416 (20%), 386 (25%), 285 (85%), 256 (48%), 159 (85%), 103 (50%), 77 (30%); $[\alpha]_D^{20}$ = −18 (c 0.02, CH_2Cl_2).

4.14. Methyl (1′*S*,2′*S*,7a′*R*,11*R*)-1′-methyl-1′,2′,5′,6′,7′,7a′-hexahydrospiro[indeno[1,2-*b*]quinoxaline-11,3′-pyrrolizine]-2′-car boxylate 8b

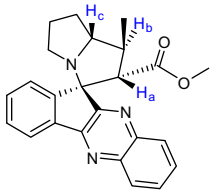

Yellow solid (373 mg, 97%); IR (KBr) (ν_{max}/cm^{-1}): CO 1724; ^{1}H NMR (300 MHz, $CDCl_3$): δ_H (ppm) = 1.30 (d, 3H, J = 6.3 Hz), 1.65–1.77 (m, 1H, pyrrolizine), 1.90–1.99 (m, 2H, pyrrolizine), 2.13–2.23 (m, 1H, pyrrolizine), 2.45–2.49 (m, 2H, pyrrolizine), 2.69–2.80 (dd, 1H, H_b), 2.91 (S, 3H, OCH_3), 3.85–3.90 (m, 1H, H_c), 3.94 (d, 1H, J = 12 Hz, H_a), 7.53–8.29 (m, **8H**, Ar); ^{13}C NMR (75 MHz, $CDCl_3$): δ_c (ppm) = 16.8, 28.4, 29.6, 31.6, 41.4, 47.7, 51.0, 72.4, 75.3, 122.3, 126.7, 128.7, 128.9, 129.3, 129.5, 129.9, 130.8, 138.0, 142.4, 142.8, 144.4, 170.5; MS m/z (%): 385(M) (45%), 354 (33%), 326 (66%), 230 (80%), 131 (24%), 91 (88%); $[\alpha]_D^{20}$ = −17 (c 0.02, CH_2Cl_2).

4.15. Methyl (1′*R*,2′*S*,7a′*R*,11*R*)-7,8-dimethyl-1′-phenyl-1′,2′,5′,6′,7′,7a′-hexahydrospiro[indeno[1,2-*b*]quinoxaline-11,3′-pyrrolizine]-2′-carboxylate 8c

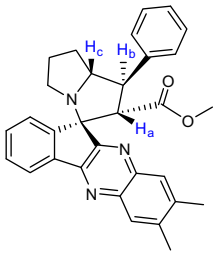

Yellow solid (458 mg, 97%); IR (KBr) (ν_{max}/cm^{-1}): CO 1720; ^{1}H NMR (300 MHz, $CDCl_3$): δ_H (ppm) = 1.83–2.28 (m, 4H, pyrrolizine), 2.56–2.69 (m, 2H, pyrrolizine), 2.64 (S, 6H, $2CH_3$), 2.87 (S, 3H, OCH_3), 3.89–3.96 (dd, 1H, H_b), 4.38–4.46 (m, 1H, H_c), 4.60 (d, 1H, J = 12 Hz, H_a), 7.27–8.34 (m, 11H, Arom); ^{13}C NMR (75 MHz, $CDCl_3$): δ_c (ppm) = 20.3, 20.3, 28.1, 31.9, 47.8, 51.1, 52.8, 63.1, 73.2, 75.2, 122.0,122.1, 127.0, 127.8, 127.9, 128.1, 128.2, 128.4, 128.7, 129.2, 129.3, 129.7, 129.9, 130.5, 138.4, 139.2, 139.8, 140.1, 141.3, 141.6, 143.9, 152.3, 163.4, 170.0; MS m/z (%): 476 (M + 1) (22%), 444 (65%), 416 (42%), 230 (50%), 131(35%), 77 (68%); $[\alpha]_D^{20}$ = −23.4 (c 0.02, CH_2Cl_2).

4.16. Methyl (1′*S*,2′*S*,7a′*R*,11*R*)-1′,7,8-trimethyl-1′,2′,5′,6′,7′,7a′-hexahydrospiro[indeno[1,2-*b*]quinoxaline-11,3′-pyrrolizine]-2′-carboxylate 8d

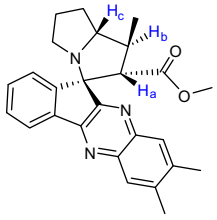

Yellow solid (327 mg, 95%); IR (KBr) (ν_{max}/cm^{-1}): CO 1733; ^{1}H NMR (300 MHz, $CDCl_3$): δ_H (ppm) = 1.29 (d, 3H, J = 6.3 Hz), 1.61–1.96 (m, 2H, pyrrolizine), 2.13–2.28 (m, 2H, pyrrolizine), 2.13 (S, 6H), 2.44–2.48 (m, 1H, pyrrolizine), 2.64–2.68 (m, 1H, H_b), 2.74 (S, 3H, OCH_3), 3.55–3.70 (m, 1H, H_c), 3.74 (d, 1H, J = 12 Hz, H_a), 7.45–8.28 (m, 6H, Ar); ^{13}C NMR (75 MHz, $CDCl_3$): δ_c (ppm) = 16.8, 20.2, 20.2, 23.3, 24.9, 26.4, 37.1, 43.6, 45.0, 46.4, 57.3, 67.8, 116.9, 117.8, 120.5, 123, 123.3, 125.8, 126.7, 127.4, 131.1, 137.1, 152.8, 170.0; MS m/z (%): 413 (M) (16%), 382 (25%), 354 (65%), 131 (35%), 91 (18%); $[\alpha]_D^{20}$ = −20.2 (c 0.03, CH_2Cl_2).

4.17. Methyl (1′*R*,2′*S*,6′*R*,7a′*R*,11*R*)-6′-hydroxy-1′-phenyl-1′,2′,5′,6′,7′,7a′-hexahydrospiro[indeno[1,2-*b*]quinoxaline-11,3′-pyrrolizine]-2′-carboxylate 8e

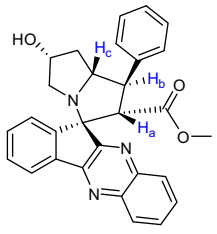

Yellow liquid (382 mg, 83%); IR (KBr) (ν_{max}/cm^{-1}): CO 1744, 3341; ^{1}H NMR (300 MHz, $CDCl_3$): δ_H (ppm) = 1.27–1.61 (m, 4H, pyrrolizine), 3.83 (S, 3H, OCH_3), 4.71 (m, 1H, pyrrolizine), 6.43–6.49 (m, 1H, H_b), 6.61 (d, 1H, H_a), 7.07–7.11 (m, 1H, H_c), 7.27–7.74 (m, 13H, Ar); ^{13}C NMR (75 MHz, $CDCl_3$): δ_c (ppm) = 40.3, 40.9, 51.2, 53.0, 54.4, 55.8, 62.7, 63.1, 74.5, 122.4, 122.6, 126.5, 127.1, 128.0, 128.4, 128.7, 128.9, 129.1, 129.4, 129.6, 129.8, 130.0, 131.1,137.7, 139.3, 139.4, 142.1, 142.3, 165.1, 170.6; MS m/z (%): 463 (M) (22%), 404 (45%), 328 (75%), 217 (33%), 129 (45%), 91 (55%); $[\alpha]_D^{20}$ = −14 (c 0.03, CH_2Cl_2).

4.18. Methyl (1′*R*,2′*S*,6′*R*,7a′*R*,11*R*)-6′-hydroxy-7,8-dimethyl-1′-phenyl-1′,2′,5′,6′,7′,7a′-hexahydrospiro[indeno[1,2-*b*]quinoxaline-11,3′-pyrrolizine]-2′-carboxylate 8f

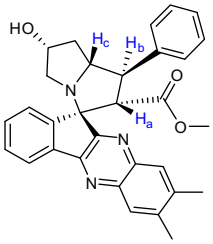

Yellow liquid (408 mg, 84%); IR (KBr) (ν_{max}/cm^{-1}): CO 1748, 3332; ^{1}H NMR (300 MHz, $CDCl_3$): δ_H (ppm) = 1.27–1.41 (m, 1H, pyrrolizine), 2.10 (S, 6H), 1.81–2.21 (m, 4H, pyrrolizine), 2.51–2.68 (m, 1H, pyrrolizine), 2.73 (S, 3H, OCH_3), 6.33–6.49 (m, 1H, H_b), 7.09 (d, 1H, H_a), 6.90–7.14 (m, 1H, H_c), 7.26–8.34 (m, 11H, Ar); ^{13}C NMR (75 MHz, $CDCl_3$): δ_c (ppm) = 20.1, 20.2, 37.5, 54.3, 55.1, 57.4, 65.6, 70.2, 72.4, 75.3, 122.0, 125.9, 127.1, 127.2, 128.7, 128.8, 128.9, 128.3, 130.5, 131.0, 131.2, 134.5, 135.0, 140.1, 142.2, 153.2, 172.4; MS m/z (%): 490 (M + 1) (25%), 432 (33%), 356 (24%), 157 (44%), 91 (64%); $[\alpha]_D^{20}$ = −18 (c 0.03, CH_2Cl_2).

4.19. Methyl (1′*S*,2′*S*,6′*R*,7a′*R*,11*R*)-6′-hydroxy-1′-methyl-1′,2′,5′,6′,7′,7a′-hexahydrospiro[indeno[1,2-*b*]quinoxaline-11,3′-pyrrolizine]-2′-carboxylate 8g

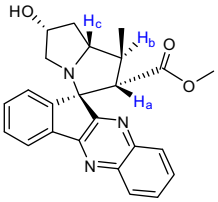

Yellow liquid (332 mg, 83%); IR (KBr) (ν_{max}/cm^{-1}): CO 1740, 3344; ^{1}H NMR (300 MHz, $CDCl_3$): δ_H (ppm) = 1.34 (d, 3H, J = 9.6 Hz, CH_3), 1.87–2.70 (m, 4H, pyrrolizine) 2.83 (S, 3H, OCH_3), 2.71–2.95 (m, 1H, pyrrolizine), 3.63–3.81 (m, 1H, H_b), 5.19–5.22 (m, 1H, H_c), 6.43 (d, 1H, H_a), 7.58–8.24 (m, **8H**, Ar); ^{13}C NMR (75 MHz, $CDCl_3$): δ_c (ppm) = 16.1, 37.0, 39.2, 55.0, 56.4, 59.7, 65.7, 69.1, 72.7, 75.2, 122.9, 125.7, 127.3, 128.6, 128.9, 129.3, 130.4, 130.8, 131.3, 135.1, 135.6, 141.8, 152.2, 173.5; MS m/z (%): 401 (M) (12%), 344 (28%), 317 (42%), 217 (60%), 91(75%); $[\alpha]_D^{20}$ = −16.4 (c 0.03, CH_2Cl_2).

4.20. Methyl (3′*S*,4′*R*,11*R*)-1′-methyl-4′-phenylspiro[indeno-[1,2-*b*]quinoxaline-11,2′-pyrrolidine]-3′-carboxylate 8h

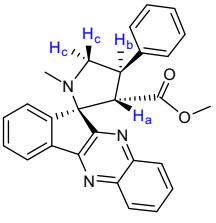

Yellow liquid (404 mg, 96%); IR (KBr) (ν_{max}/cm^{-1}): CO 1738; ^{1}H NMR (300 MHz, $CDCl_3$): δ_H (ppm) = 1.99 (S, 3H), 2.93 (S, OCH_3), 3.62–3.68 (t, 1H, H_c), 3.82–3.88 (t, 1H, H_c), 4.11 (d, 1H, J = 9.8 Hz, H_a), 4.36–4.45 (m, 1H, H_b), 7.28–8.44 (m, 13H, Ar); ^{13}C NMR (75 MHz, $CDCl_3$): δ_c (ppm) = 35.4, 45.3, 50.9, 51.1, 61.3, 61.8, 121.6, 121.5, 125.1, 126.5, 128.6, 128.7, 128.8, 130.4, 131.4, 131.1, 137.2, 141.7, 142.3, 171.2; MS m/z (%): 379 (M-41) (35%), 217 (80%), 91 (44%), 77 (86%); $[\alpha]_D^{20}$ = −34 (c 0.03, CH_2Cl_2).

4.21. Methyl (3′*S*,4′*S*,11*R*)-1′,4′-dimethylspiro[indeno[1,2-*b*]quinoxaline-11,2′-pyrrolidine]-3′-carboxylate 8i

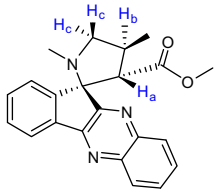

Yellow liquid (330 mg, 92%); IR (KBr) (ν_{max}/cm^{-1}): CO 1737; ^{1}H NMR (300 MHz, $CDCl_3$): δ_H (ppm) = 1.44 (S, 3H), 2.11 (S, 3H), 2.85 (S, OCH_3), 3.50–3.68 (t, 2H, H_c), 3.75 (d, 1H, J = 9.9 Hz, H_a), 4.27–4.48 (m, 1H, H_b), 7.27–8.28 (m, **8H**, Ar); ^{13}C NMR (75 MHz, $CDCl_3$): δ_c (ppm) = 16.1, 36.2, 38.3, 55.3, 60.1, 63.3, 73.0, 121.3, 122.6, 125.1, 126.9, 128.1, 128.4, 128.7, 130.3, 131.8, 131.9, 137.1, 141.8, 173.3; MS m/z (%): 359 (M) (32%), 317 (20%), 300 (43%), 217 (86%), 91 (75%); $[\alpha]_D^{20}$ = −33 (c 0.03, CH_2Cl_2).

References

1. Ramon, D. J.; Yus, M. *Angew. Chem., Int. Ed.* **2005**, *44*, 1602–1634.
2. (a) Gothelf, K. V.; Jørgensen, K. A. *Chem. Rev.* **1998**, *98*, 863–909; (b) Karlsson, S.; Högberg, H. E. *Org. Prep. Proced. Int.* **2001**, *33*, 103–172.
3. Gothelf, K. V.; Jørgensen, K. A. In *Synthetic Applications of 1,3-Dipolar Cycloaddition Chemistry Toward Heterocycles and Natural Products*; Padwa, A., Pearson, W. H., Eds.; John Wiley & Sons Inc: New York, 2002; Vol. 59, pp 851–860.
4. (a) Evans, D. A.; Takacs, J. M.; McGee, L. R.; Ennis, M. D.; Mathre, D. J.; Bartroli, J. *Pure Appl. Chem.* **1981**, *53*, 1109–1127; (b) Evans, D. A. *Aldrichimica Acta* **1982**, *15*, 23–32; (c) Ager, D. J.; Prakash, I.; Schaad, D. R. *Chem. Rev.* **1996**, *96*, 835–875; (d) Ager, D. J.; Prakash, I.; Schaad, D. R. *Aldrichimica Acta* **1997**, *30*, 3–14.
5. Shi, F.; Mancuso, R.; Larock, R. C. *Tetrahedron Lett.* **2009**, *50*, 4067–4070.
6. Pearson, W. H. In *Studies in Natural Product Chemistry*; Rahman, A. U., Ed.; Elsevier: Amsterdam, 1998; Vol. 1, pp 323–358.
7. (a) Hartmann, T.; Witte, L. Chemistry, Biology and Chemoecology of Pyrrolizidine Alkaloids In Alkaloids In *Chemical and Biological Perspectives*; Pelletier, S. W., Ed.; Pergamon Press: Oxford, UK, 1995; Vol. 9, pp 155–233; (b) Monlineux, R. J. In Alkaloids. In *Chemical and Biological Perspective*; Pelletier, S. W., Ed.; Wiley: New York, 1987. Chapter 1; (c) Jiang, H.; Zhao, J.; Han, X.; Zhu, S. *Tetrahedron* **2006**, *62*, 11008–11011; (d) Abou-Gharbia, M. A.; Doukas, P. H. *Heterocycles* **1979**, *12*, 637–640; (e) Kornett, M. J.; Thio, A. P. *J. Med. Chem.* **1976**, *19*, 892–898; (f) Lundahl, K.; Schut, J.; Schlatmann, J. L. M. A.; Paerels, G. B.; Peters, A. *J. Med. Chem.* **1972**, *15*, 129–132.
8. (a) Dai, W.-M.; Nagao, Y.; Fujita, E. *Heterocycles* **1990**, *30*, 1231–1261; (b) Smith, L. W.; Culvenor, C. C. J. *J. Nat. Prod.* **1981**, *44*, 129–152; (c) Coulombe, J. R. A. *Adv. Food Nutr. Res.* **2003**, *45*, 61–99; (d) Li, N.; Xia, Q.; Ruan, J.; Fu, P. P.; Lin, G. *Curr. Drug Metab.* **2011**, *12*, 823–834.
9. (a) Danylkova, N. O.; Alcala, S. R.; Pomeranz, H. D.; McLoon, L. K. *Exp. Eye Res.* **2007**, *84*, 293–301; (b) Mohanasundaram, U. M.; Chitkara, R.; Krishna, G. *Int. J. Chron. Obstruct. Pulmon. Dis.* **2008**, *3*, 239–251; (c) Klesges, R. C.; Johnson, K. C.; Somes, G. *JAMA* **2006**, *296*, 94–95; (d) Baffert, F.; Régnier, C. H.; De Pover, A.; Pissotsoldermann, C.; Tavares, G. A.; Blasco, F.; Brueggen, J.; Chéne, P.; Drueckes, P.; Erdmann, D.; Furet, P.; Gerspacher, M.; Lang, M.; Ledieu, D.; Nolan, L.; Ruetz, S.; Trappe, J.; Vangrevelinghe, E.; Wartmann, M.; Wyder, L.; Hofmann, F.; Radimerski, T. *Mol. Cancer Ther.* **2010**, *9*, 1945–1955; (e) Simeonov, A.; Yasgar, A.; Jadhav, A.; Lokesh, G. L.; Klumpp, C.; Michael, S.; Austin, C. P.; Natarajan, A.; Inglese, J. *Anal. Biochem.* **2008**, *375*, 60–70; (f) Undevia, S. D.; Innocenti, F.; Ramirez, J.; House, L.; Desai, A. A.; Skoog, L. A.; Singh, D. A.; Karrison, T.; Kindler, H. L.; Ratain, M. J. *Eur. J. Biol. Cancer.* **2008**, *44*, 1684–1692.
10. (a) Mohammadizadeh, M. R.; Firoozi Moemeni, N. *Bull. Korean. Chem. Soc.* **2009**, *30*, 1877–1889; (b) Arvinnezhad, H.; Samadi, S.; Tajbakhsh, M.; Jadidi, K.; Khavasi, H. R. J. *J. Heterocycl. Chem.* **2012**, *49*, 190–194; (c) Taghizadeh, M. J.; Arvinnezhad, H.; Samadi, S.; Jadidi, K.; Javidan, A.; Notash, B. *Tetrahedron Lett.* **2012**, *53*, 5148–5150; (d) Mehrdad, M.; Faraji, L.; Jadidi, K.; Eslami, P.; Sureni, H. *Monatsh. Chem.* **2011**, *142*, 917–921; (e) Faraji, L.; Arvinnezhad, H.; Alikami, N.; Jadidi, K. *Lett. Org. Chem.* **2010**, *7*, 472–474; (f) Jadidi, K.; Gharemanzadeh, R.; Mehrdad, M.; Darabi, H. R.; Khavasi, H. R.; Asgari, D. *Ultrason. Sonochem.* **2008**, *15*, 124–128; (g) Jadidi, K.; Moghaddam, M. M.; Aghapoor, K.; Gharemanzadeh, R. *J. Chem. Res.* **2007**, 71–73; (h) Azizian, J.; Jadidi, K.; Mehrdad, M.; Sarrafi, Y. Q. *Synth. Commun.* **2000**, *30*, 2309–2315; (i) Azizian, J.; Morady, A. V.; Jadidi, K.; Mehrdad, M.; Sarrafi, Y. *Synth. Commun.* **2000**, *30*, 537–542; (j) Salahi, F.; Taghizadeh, M. J.; Arvinnezhad, H.; Moemeni, M.; Jadidi, K.; Notash, B. *Tetrahedron Lett.* **2014**, *55*, 1515–1518.
11. (a) Sibi, M.; Stanley, L.; Jasperse, C. *J. Am. Chem. Soc.* **2005**, *127*, 8276–8277; (b) Michael, T.; Crimmins, M.; Hamish, S.; Colin, O.; Hughes, C. *Org. Synth.* **2011**, *88*, 364–376.
12. X-ray data for **7d:** $C_{35}H_{34}N_4O_3$, M = 558.66, Orthorhombic system, space group $P2_12_12_1$, a = 12.287(3), b = 14.033(3), c = 16.500(3) Å; V = 2845.0(11) Å^3, Z = 4, D_{calcd} = 1.304 g cm^{-3}, μ(Mo-Kα) = 0.084 mm^{-1}, crystal dimension of 0.52×0.23×0.20 mm. The X-ray diffraction measurement was made on a STOE IPDS 2T diffractometer with graphite monochromated Mo-Kα radiation. The structure was solved by using SHELXS. The Data reduction and structure refinement was carried out with SHELXL using the X-STEP32 crystallographic software package. [13] The non-hydrogen atoms were refined anisotropically by full matrix least-squares on F^2 values to final R_1 = 0.0860, wR_2 = 0.1250 and S = 1.061 with 383 parameters using 4901 independent reflection (θ range = 2.53-25°). Hydrogen atoms were added in idealized positions. The crystallographic information file has been deposited with the Cambridge Data Centre, CCDC 1033398.
13. X-STEP32 Version 1.07b, Crystallographic Package; Stoe & Cie GmbH: Darmstadt, Germany, 2000.
14. Kanomata, N.; Maruyama, S.; Tomono, K.; Anada, S. *Tetrahedron Lett.* **2003**, *44*, 3599–3603.
15. (a) Becke, A. D. *J. Chem. Phys.* **1993**, *98*, 5648–5652; (b) Lee, C.; Yang, W.; Parr, R. G. *Phys. Rev. B* **1988**, *37*, 785–789.
16. (a) Sarrafi, Y.; Sadatshahabi, M.; Hamzehloueian, M.; Alimohammadi, K.; Tajbakhsh, M. *Synthesis* **2013**, *45*, 2294–2304; (b) Alimohammadi, K.; Sarrafi, Y.; Tajbakhsh, M.; Yeganegi, S.; Hamzehloueian, M. *Tetrahedron* **2011**, *67*, 1589–1597; (c) Sarrafi, Y.; Hamzehloueian, M.; Alimohammadi, K.; Yeganegi, S. *J. Mol. Struct.* **2012**, *1030*, 168–176; (d) Gérard, H.; Chataigner, I. *J. Org. Chem.* **2013**, *78*, 9233–9242; (e) Domingo, L. R.; Saéz, J. A.; Zaragozá, R. J.; Arno, M. *J. Org. Chem.* **2008**, *73*, 8791–8799; (f) Boz, E.; Tüzün, N. S. *J. Organomet. Chem.* **2013**, *724*, 167–176; (g) Wang, H.; Jain, P.; Antilla, J. C.; Houk, K. N. *J. Org. Chem.* **2013**, *78*, 1208–1215; (h) Bentabed-Ababsa, G.; Derdour, A.; Roisnel, T.; Sáez, J. A.; Pérez, P.; Chamorro, E.; Domingo, L. R.; Mongin, F. *J. Org. Chem.* **2009**, *74*, 2120–2133.
17. (a) Reed, A. E.; Weinstock, R. B.; Weinhold, F. *J. Chem. Phys.* **1985**, *83*, 735–746; (b) Reed, A. E.; Curtiss, L. A.; Weinhold, F. *Chem. Rev.* **1988**, *88*, 899–926.
18. Frisch, M. J.; Trucks, G. W.; Schlegel, H. B.; Scuseria, G. E.; Robb, M. A.; Cheeseman, J. R.; Scalmani, G.; Barone, V.; Mennucci, B.; Petersson, G. A.; Nakatsuji, H.; Caricato, M.; Li, X.; Hratchian, H. P.; Izmaylov, A. F.; Bloino, J.; Zheng, G.; Sonnenberg, J. L.; Hada, M.; Ehara, M.; Toyota, K.; Fukuda, R.; Hasegawa, J.; Ishida, M.; Nakajima, T.; Honda, Y.; Kitao, O.; Nakai, H.; Vreven, T., Jr.; Montgomery, J. A.; Peralta, J. E.; Ogliaro, F.; Bearpark, M.; Heyd, J. J.; Brothers, E.; Kudin, K. N.; Staroverov, V. N.; Kobayashi, R.; Normand, J.; Raghavachari, K.; Rendell, A.; Burant, J. C.; Iyengar, S. S.; Tomasi, J.; Cossi, M.; Rega, N.; Millam, N. J.; Klene, M.; Knox, J. E.; Cross, J. B.; Bakken, V.; Adamo, C.; Jaramillo, J.; Gomperts, R.; Stratmann, R. E.; Yazyev, O.; Austin, A. J.; Cammi, R.; Pomelli, C.; Ochterski, J. W.; Martin, R. L.; Morokuma, K.; Zakrzewski, V. G.; Voth, G. A.; Salvador, P.; Dannenberg, J. J.; Dapprich, S.; Daniels, A. D.; Farkas, Ö.; Foresman, J. B.; Ortiz, J. V.; Cioslowski, J.; Fox, D. J. *Gaussian 09, Revision A.1*; Gaussian, Inc.: Wallingford CT, 2009.
19. (a) Borden, W. T.; Loncharich, R. J.; Houk, K. N. *Annu. Rev. Phys. Chem.* **1988**, *39*, 213–236; (b) Moyano, A.; Pericàs, M. A.; Valentí, E. *J. Org. Chem.* **1989**, *54*, 573–582; (c) Cossío, F. P.; Morao, I.; Jiao, H.; Schleyer, P. V. R. *J. Am. Chem. Soc.* **1999**, *121*, 6737–6746; (d) Morao, I.; Lecea, B.; Cossío, F. P. *J. Org. Chem.* **1997**, *62*, 7033–7036; (e) Lecea, B.; Arrieta, A.; Roa, G.; Ugalde, J. M.; Cossío, F. P. *J. Am. Chem. Soc.* **1994**, *116*, 9613–9619; (f) Lecea, B.; Arrieta, A.; Lopez, X.; Ugalde, J. M.; Cossío, F. P. *J. Am. Chem. Soc.* **1995**, *117*, 12314–12321; (g) Arrieta, A.; Otaegui, D.; Zubia, A.; Cossío, F. P.; Diaz-Ortiz, A.; Hoz, A.; Herrero, M. A.; Prieto, P.; Foces, C. F.; Pizarro, J. L.; Arriortua, M. I. *J. Org. Chem.* **2007**, *72*, 4313–4322.
20. Wiberg, K. B. *Tetrahedron* **1968**, *24*, 1083–1096.
21. (a) Parr, R. G.; Pearson, R. G. *J. Am. Chem. Soc.* **1983**, *105*, 7512–7516; (b) Parr, R. G.; Yang, W. *Density Functional Theory of Atoms and Molecules*; Oxford University: New York, NY, 1989.
22. Parr, R. G.; Szentpaly, L. V.; Liu, S. *J. Am. Chem. Soc.* **1999**, *121*, 1922–1924.
23. Domingo, L. R.; Chamorro, E.; Pérez, P. *J. Org. Chem.* **2008**, *73*, 4615–4624.
24. (a) Domingo, L. R.; Aurell, M. J.; Perez, P.; Contreras, R. *Tetrahedron* **2002**, *58*, 4417–4423; (b) Domingo, L. R.; Asensio, A.; Arroyo, P. *J. Phys. Org. Chem.* **2002**, *15*, 660–666; (c) Domingo, L. R.; Arno, M.; Contreras, R.; Perez, P. *J. Phys. Chem.* **2002**, *106*, 952–961; (d) Domingo, L. R. *Tetrahedron* **2002**, *58*, 3765–3774; (e) Domingo, L. R.; Aurell, M. J. *J. Org. Chem.* **2002**, *67*, 959–965; (f) Domingo, L. R.; Aurell, M. J.; Perez, P.; Contreras, R. *J. Org. Chem.* **2003**, *68*, 3884–3890; (g) Domingo, L. R.; Andres, J. *J. Org. Chem.* **2003**, *68*, 8662–8668; (h) Parr, R. G.; Yang, W. *J. Am. Chem. Soc.* **1984**, *106*, 4049–4050.

Please cite this article in press as: Shahrestani, N.; et al. *Tetrahedron: Asymmetry* (2015), http://dx.doi.org/10.1016/j.tetasy.2015.08.013

ARTICLE IN PRESS

25. (a) Sustmann, R. *Tetrahedron Lett.* **1971**, 2717–2720; (b) Sustmann, R.; Trill, H. *Tetrahedron Lett.* **1972**, 4271–4274; (c) Sustmann, R. *Pure Appl. Chem.* **1974**, *40*, 569–593; (d) Sustmann, R. *Tetrahedron Lett.* **1971**, 2721–2724.
26. (a) Chandra, A. K.; Nguyen, M. T. *J. Phys. Chem. A* **1998**, *102*, 6181–6185; (b) Nguyen, T. L.; De Proft, F.; Chandra, A. K.; Uchimaru, T.; Nguyen, M. T.; Geerlings, P. *J. Org. Chem.* **2001**, *66*, 6096–6103; (c) Sengupta, D.; Chandra, A. K.; Nguyen, M. T. *J. Org. Chem.* **1997**, *62*, 6404–6406; (d) Damoun, S.; Van de Woude, G.; Mendez, F.; Geerlings, P. *J. Phys. Chem. A* **1997**, *101*, 886–893; (e) Chandra, A. K.; Nguyen, M. T. *Int. J. Mol. Sci.* **2002**, *3*, 310–323.
27. Chermette, H. *J. Comput. Chem.* **1999**, *20*, 129–154.

Please cite this article in press as: Shahrestani, N.; et al. *Tetrahedron: Asymmetry* (2015), http://dx.doi.org/10.1016/j.tetasy.2015.08.013